

Iron–Iridium Mixed-metal Carbonyl Clusters. Part 2.¹ Synthesis and Chemical Behaviour of the Tetranuclear Complexes $[\text{FeIr}_3(\text{CO})_{12}]^-$, $[\text{Fe}_2\text{Ir}_2(\text{CO})_{12}]^{2-}$, $[\text{Fe}_2\text{Ir}_2\text{H}(\text{CO})_{12}]^-$, and $[\text{Fe}_3\text{Ir}(\text{CO})_{13}]^-$. Solid-state Structures of $[\text{N}(\text{PPh}_3)_2][\text{FeIr}_3(\text{CO})_{12}]$, $[\text{NEt}_4]_2[\text{Fe}_2\text{Ir}_2(\text{CO})_{12}]$, and $[\text{PPh}_4][\text{Fe}_2\text{Ir}_2(\text{CO})_{12}]\{\mu_3\text{-Au}(\text{PPh}_3)\}^\dagger$

Roberto Della Pergola* and Luigi Garlaschelli

Dipartimento di Chimica Inorganica e Metallorganica, Universita' di Milano, via G. Venezian 21, I-20133 Milano, Italy

Francesco Demartin,* Mario Manassero, Norberto Masciocchi, and Mirella Sansoni

Istituto di Chimica Strutturistica Inorganica, Universita' di Milano, via G. Venezian 21, I-20133 Milano, Italy

The compound $[\text{FeIr}_3(\text{CO})_{12}]^-$ can be obtained by degradation of $[\text{FeIr}_4(\text{CO})_{15}]^{2-}$ under a carbon monoxide atmosphere as well as by reduction of an equimolar mixture of $[\text{Fe}(\text{CO})_5]$ and $[\text{Ir}_4(\text{CO})_{12}]$ in alcoholic NaOH under 1 atm (101 325 Pa) of carbon monoxide. The salt $[\text{N}(\text{PPh}_3)_2][\text{FeIr}_3(\text{CO})_{12}]$ (**1**) crystallizes in the monoclinic space group $P2_1/c$ with unit-cell dimensions $a = 14.968(2)$, $b = 19.892(2)$, $c = 16.610(2)$ Å, $\beta = 96.10(2)^\circ$, and $Z = 4$. The molecular structure of the anion consists of a tetrahedron of metal atoms surrounded by twelve carbonyl groups: nine are terminally bound whereas three are bridging the edges of the FeIr_2 basal face. Average bond distances are Ir–Ir 2.696, Ir–Fe 2.682, Ir–CO_t 1.889, Fe–CO_t 1.729, Ir–CO_b 2.154, and Fe–CO_b 1.887 Å (b = bridging, t = terminal). The dianion $[\text{Fe}_2\text{Ir}_2(\text{CO})_{12}]^{2-}$ (**2**) was obtained by several different ways, the most selective being the condensation of $[\text{Fe}_2(\text{CO})_9]$ with $[\text{Ir}(\text{CO})_4]^-$. The salt $[\text{NEt}_4]_2[\text{Fe}_2\text{Ir}_2(\text{CO})_{12}]$ (**2**) crystallizes in the monoclinic space group $P2_1$ with $a = 9.072(5)$, $b = 19.910(5)$, $c = 10.094(3)$ Å, $\beta = 91.92(3)^\circ$, and $Z = 2$. The molecular structure of the dianion is based on a tetrahedral cluster of metal atoms and consists of an apical $\text{Ir}(\text{CO})_3$ group co-ordinated by three metal–metal bonds to a basal $\text{Fe}_2\text{Ir}(\text{CO})_9$ fragment containing two $\text{Fe}(\text{CO})_2$ units and one $\text{Ir}(\text{CO})_2$ group linked to each other by a metal–metal bond and bridging carbonyl groups. Selected distances are: Ir–Ir 2.734(1), Fe–Fe 2.581(2), and averages Ir–Fe 2.683, Ir–CO_t 1.863, Fe–CO_t 1.722, Ir–CO_b 2.142, and Fe–CO_b 1.947 Å. The salt $[\text{PPh}_4][\text{Fe}_2\text{Ir}_2(\text{CO})_{12}]\{\mu_3\text{-Au}(\text{PPh}_3)\}$ (**3**) which crystallizes in the monoclinic space group $P2_1/c$ with $a = 10.990(3)$, $b = 13.693(2)$, $c = 35.883(3)$ Å, $\beta = 97.39(2)^\circ$, and $Z = 4$. The metal framework of the anion is a trigonal bipyramid with the $\text{Au}(\text{PPh}_3)$ moiety in one of the apical positions, the other being occupied by a $\text{Fe}(\text{CO})_3$ group. Each edge of the equatorial triangle, formed by one iron and two iridium atoms, is spanned by a bridging carbonyl ligand, and two terminal CO groups are attached to each metal of this triangle. Selected bond distances are: Ir–Ir 2.758(1), and averages Ir–Fe 2.710, Ir–Au 2.786, Fe–Au 2.806(1), Ir–CO_t 1.845, Fe–CO_t 1.776, Ir–CO_b 2.113, and Fe–CO_b 1.996 Å.

Recently we reported the preparation, reactivity, and solid-state structures of two pentanuclear clusters, $[\text{N}(\text{PPh}_3)_2][\text{FeIr}_4(\text{CO})_{15}]$ and $[\text{PPh}_4][\text{Fe}_2\text{Ir}_3(\text{CO})_{14}]$.¹ In that paper we also reported the existence of other mixed-metal carbonyl clusters, namely $[\text{FeIr}_3(\text{CO})_{12}]^-$ (**1**) and a brown derivative with no definitive formulation. Anion (**1**) is obtained when the pentanuclear carbonyl cluster $[\text{FeIr}_4(\text{CO})_{15}]^{2-}$ is kept under a carbon monoxide atmosphere and was tentatively formulated on the basis of elemental analysis and i.r. data. The brown complex was prepared by redox condensation of several metal carbonyl complexes of Fe and Ir and all attempts to obtain

single crystals of good quality for X-ray analysis of this species, in combination with different counter cations, failed.¹ However, several analytical data suggested the formulation $[\text{Fe}_2\text{Ir}_2(\text{CO})_{12}]^{2-}$.

We have now extended the study on mixed Fe–Ir carbonyl clusters and in this paper we describe the syntheses and the chemical characterization of $[\text{FeIr}_3(\text{CO})_{12}]^-$ (**1**), $[\text{Fe}_2\text{Ir}_2(\text{CO})_{12}]^{2-}$ (**2**), $[\text{Fe}_2\text{Ir}_2(\text{CO})_{12}]\{\mu_3\text{-Au}(\text{PPh}_3)\}^-$ (**3**), $[\text{Fe}_2\text{Ir}_2\text{H}(\text{CO})_{12}]^-$ (**4**), and $[\text{Fe}_3\text{Ir}(\text{CO})_{13}]^-$ (**5**). The solid-state structures of $[\text{N}(\text{PPh}_3)_2][\text{FeIr}_3(\text{CO})_{12}]$, $[\text{NEt}_4]_2[\text{Fe}_2\text{Ir}_2(\text{CO})_{12}]$, and $[\text{PPh}_4][\text{Fe}_2\text{Ir}_2(\text{CO})_{12}]\{\mu_3\text{-Au}(\text{PPh}_3)\}$ are also reported.

† Bis(triphenylphosphine)iminium 1,2;1,4;2,4-tri- μ -carbonyl-1,1,2,2-3,3,3,4,4-nonacarbonyl-tetrahedro-1,2,3-tri-iridium-4-ferrate, bis(tetraethylammonium) 1,3;1,4;2,4-tri- μ -carbonyl-1,1,2,2,2,3,3,4,4-nonacarbonyl-tetrahedro-1,2-di-iridium = 3,4-diferrate, and tetraphenylphosphonium 1,2,3- μ_3 -bis(triphenylphosphine)aurio-1,2;1,3;2,3-tri- μ -carbonyl-1,1,2,2,2,3,3,4,4-nonacarbonyl-tetrahedro-1,2-di-iridium-3,4-diferrate.

Supplementary data available: see Instructions for Authors, *J. Chem. Soc., Dalton Trans.*, 1990, Issue 1, pp. xix–xxii.

Results and Discussion

*Preparation of $[\text{FeIr}_3(\text{CO})_{12}]^-$ (**1**).—*The pentanuclear cluster $[\text{FeIr}_4(\text{CO})_{15}]^{2-}$ is easily obtained by reduction, under a carbon monoxide atmosphere, of a suspension of $[\text{Fe}(\text{CO})_5]$ and $[\text{Ir}_4(\text{CO})_{12}]$ in alcoholic NaOH. By following the reaction course using i.r. spectroscopy it is possible to detect, at the beginning, the formation of the anionic derivatives $[\text{Ir}_4\text{H}$

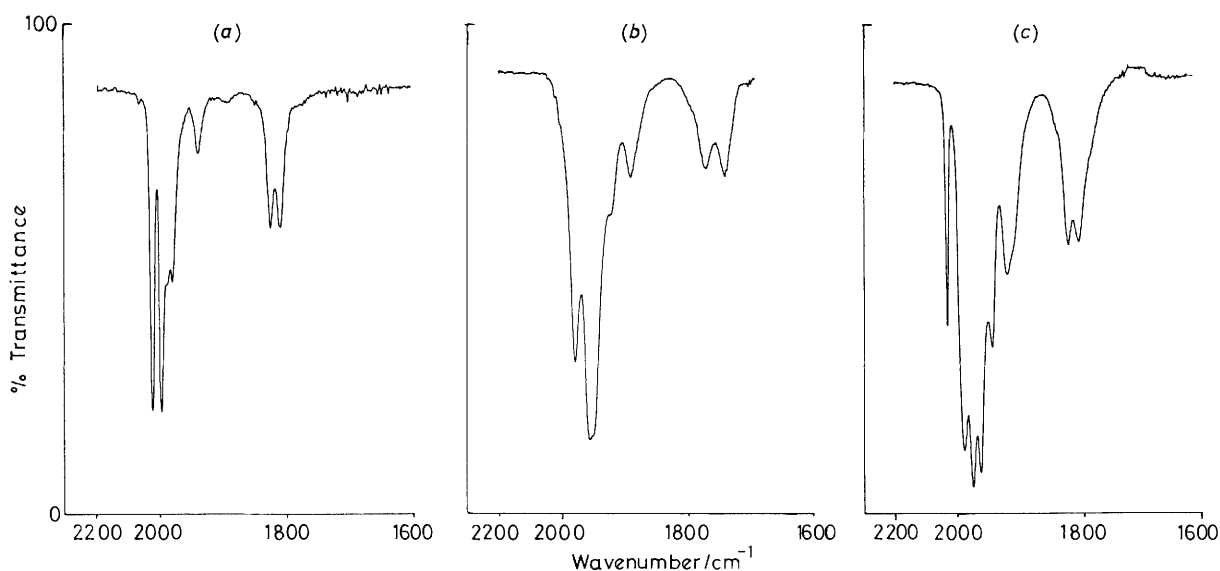
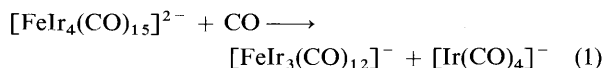


Figure 1. Infrared spectra of (a) $[\text{N}(\text{PPh}_3)_2][\text{FeIr}_3(\text{CO})_{12}]^-$ (**1**) in thf solution, (b) $[\text{N}(\text{PPh}_3)_2]_2[\text{Fe}_2\text{Ir}_2(\text{CO})_{12}]^{2-}$ (**2**) in MeCN solution, and (c) $[\text{PPh}_4][\text{Fe}_2\text{Ir}_2(\text{CO})_{12}\{\mu_3\text{-Au}(\text{PPh}_3)\}]^-$ (**3**) in thf solution

$(\text{CO})_{11}]^-$ and $[\text{FeH}(\text{CO})_4]^-$ which condense together to produce $[\text{FeIr}_4(\text{CO})_{15}]^{2-}$, and after 6 h the reaction is complete.¹ In solution $[\text{FeIr}_4(\text{CO})_{15}]^{2-}$ is not very stable either under a nitrogen or a carbon monoxide atmosphere. When $[\text{FeIr}_4(\text{CO})_{15}]^{2-}$ is not isolated from the reaction medium, the transformation of the dianion into $[\text{FeIr}_3(\text{CO})_{12}]^-$ and $[\text{Ir}(\text{CO})_4]^-$ is complete after about 5 d. The degradation of the dianion in tetrahydrofuran (thf) solution, at room temperature and under 1 atm of carbon monoxide, is very selective, producing the yellow tetranuclear compound $[\text{FeIr}_3(\text{CO})_{12}]^-$ (**1**) and the mononuclear species $[\text{Ir}(\text{CO})_4]^-$ according to the stoichiometry (1). This reaction is complete after 4 d and it is

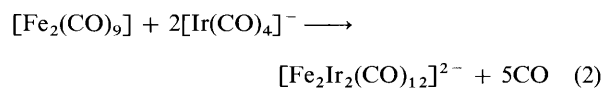


slow enough to allow the recovery of $[\text{FeIr}_4(\text{CO})_{15}]^{2-}$ in good yield by crystallization.¹ The monoanion $[\text{FeIr}_3(\text{CO})_{12}]^-$ is also obtained as a by-product when $[\text{FeIr}_4(\text{CO})_{15}]^{2-}$ is left under nitrogen, but in this case the major product is $[\text{FeIr}_4(\text{CO})_{13}]^{2-}$.² The structurally related compound $[\text{Ir}_3\text{Ru}(\text{CO})_{12}]^-$ has also been obtained by decomposition of $[\text{Ir}_4\text{Ru}(\text{CO})_{15}]^{2-}$ in the absence of CO, by subjecting the mixed-metal carbonyl cluster to a vacuum.³ In principle the direct synthesis of (**1**) is more straightforward, but the presence of Na_2CO_3 , produced during the reduction process, the excess of NaOH, and, probably, unreacted metal carbonyls makes the isolation of (**1**) quite difficult and, therefore, the intermediate isolation of $[\text{FeIr}_4(\text{CO})_{15}]^{2-}$ is more advisable. The degradation is not reversible, and an equimolar mixture of $[\text{FeIr}_3(\text{CO})_{12}]^-$ and $[\text{Ir}(\text{CO})_4]^-$, at room temperature under nitrogen, does not regenerate any trace of $[\text{FeIr}_4(\text{CO})_{15}]^{2-}$. Although in this fragmentation several different effects are probably involved (*e.g.* separation of the negative charges, release of the stereochemical hindrance, redistribution of carbon monoxide ligands on different metals with different coordination modes) the most relevant thermodynamic changes are the formation of only one metal-CO bond and the loss of three Ir-Ir bonds. The overall balance confirms the hypothesis that these metal-metal interactions in the pentanuclear cluster are very weak, as inferred from their length in the solid-state structure.^{1,4} The salts of $[\text{FeIr}_3(\text{CO})_{12}]^-$ with different bulky

cations are well soluble in thf, MeOH, CH_2Cl_2 , and acetone, sparingly soluble in 2-propanol; they can be crystallized from their thf solutions by layering cyclohexane. Complex (**1**) is indefinitely stable either under nitrogen or under carbon monoxide; in the solid state, as its $[\text{N}(\text{PPh}_3)_2]^+$ salt, it is also stable for a few days in the air. Although the solid-state structure and the chemical properties of $[\text{FeIr}_3(\text{CO})_{12}]^-$ are very similar to those of the already reported $[\text{Ir}_3\text{Ru}(\text{CO})_{12}]^-$,³ the i.r. spectrum, shown in Figure 1(a), is markedly different showing absorption bands in the CO stretching region at 2023vs, 1997vs, 1987 (sh), 1979m, 1939w, 1824m, and 1808m cm^{-1} (thf solution) recalling that of other homonuclear anionic Ir_4 clusters with the same C_s symmetry.⁵

In thf solution compound (**1**) does not react with $[\text{Au}(\text{PPh}_3)\text{Cl}]$ and cannot be protonated by addition of H_2SO_4 . Instead, all attempts to prepare the neutral derivative $[\text{FeIr}_3\text{H}(\text{CO})_{12}]$ under stronger protonating conditions, starting from a CH_2Cl_2 solution of $[\text{FeIr}_3(\text{CO})_{12}]^-$ and using $\text{CF}_3\text{CO}_2\text{H}$, failed because impure $[\text{Ir}_4(\text{CO})_{12}]$ was obtained.

*Preparation of $[\text{Fe}_2\text{Ir}_2(\text{CO})_{12}]^{2-}$ (**2**) and $[\text{Fe}_2\text{Ir}_2(\text{CO})_{12}\{\mu_3\text{-Au}(\text{PPh}_3)\}]^-$ (**3**).—*The dianion $[\text{Fe}_2\text{Ir}_2(\text{CO})_{12}]^{2-}$ (**2**) has been obtained by several synthetic routes, essentially redox condensation. Compound (**2**) can be prepared by treating a highly reduced carbonyl anion of iron with complexes of Ir^{I} or Ir^{0} , but its formation is so favoured that it can be synthesized also by reversing the oxidation states of the starting materials. Thus the best way to produce (**2**) is the reaction of $[\text{Fe}_2(\text{CO})_9]$ with $[\text{Ir}(\text{CO})_4]^-$ in refluxing acetone according to equation (2). A



small excess of $[\text{Fe}_2(\text{CO})_9]$ is required to drive the reaction to completion.

A different method to prepare $[\text{Fe}_2\text{Ir}_2(\text{CO})_{12}]^{2-}$ is the reaction between a large excess of $[\text{NEt}_4][\text{FeH}(\text{CO})_4]$ and $[\text{N}(\text{PPh}_3)_2][\text{Ir}(\text{CO})_2\text{Cl}_2]$. At room temperature, in thf solution, the reaction is quite slow and the stoichiometry approaches fairly well to equation (3). After 72 h of reaction, in solution are

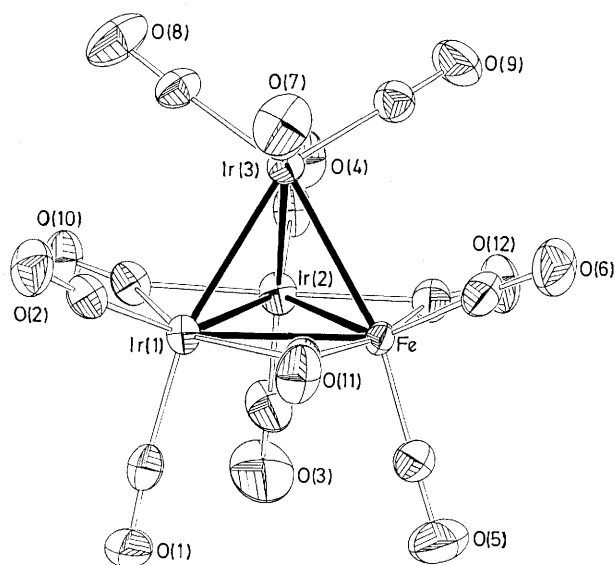
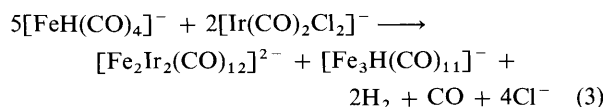


Figure 2. ORTEP drawing of the anion $[\text{FeIr}_3(\text{CO})_{12}]^{2-}$ (1)

Table 1. Selected distances (Å) and angles (°) in the monoanion $[\text{FeIr}_3(\text{CO})_{12}]^{2-}$ (1) with estimated standard deviations (e.s.d.s) on the last figure in parentheses

M-M		M-CO _b -M	
Ir(1)-Ir(2)	2.676(1)	Ir(1)-C(10)-Ir(2)	79.1(4)
Ir(1)-Ir(3)	2.700(1)	Ir(1)-C(11)-Fe	81.4(4)
Ir(1)-Fe	2.673(1)	Ir(2)-C(12)-Fe	81.5(4)
Ir(2)-Ir(3)	2.711(1)		
Ir(2)-Fe	2.691(1)	M-C-O _b	
Ir(3)-Fe	2.681(1)	Ir(1)-C(10)-O(10)	143.2(8)
		Ir(1)-C(11)-O(11)	131.2(8)
M-CO ^{a,b}		Ir(2)-C(10)-O(10)	137.6(8)
Ir-CO _t	1.889	Ir(2)-C(12)-O(12)	131.5(9)
Fe-CO _t	1.729	Fe-C(11)-O(11)	147.4(8)
Ir-CO _b	2.154	Fe-C(12)-O(12)	147.0(9)
Fe-CO _b	1.887		
C-O _t			
Fe _{bonded}	1.161		
Ir _{bonded}	1.132		
C-O _b	1.175		

^a b = Bridging, t = terminal. ^b Average values.



present $[\text{Fe}_3\text{H}(\text{CO})_{11}]^-$, some unreacted starting material, and unidentified by-products; in addition a large amount of the insoluble salt $[\text{N}(\text{PPh}_3)_2]_2[\text{Fe}_2\text{Ir}_2(\text{CO})_{12}]$ is obtained. On the contrary, in refluxing acetone the reaction is much faster (about 8 h) and almost quantitative with respect to $[\text{Ir}(\text{CO})_2\text{Cl}_2]^-$. However, a different pathway is followed and a brown compound, with properties very similar to those of $[\text{Fe}_2\text{Ir}_2(\text{CO})_{12}]^{2-}$, is obtained. The nature of this cluster is presently under investigation, but the chemical properties and the i.r. spectrum suggest the formulation $[\text{Fe}_3\text{IrH}(\text{CO})_{12}]^{2-}$. The i.r. spectrum, shown in Figure 1(b), of $[\text{N}(\text{PPh}_3)_2]_2[\text{Fe}_2\text{Ir}_2(\text{CO})_{12}]$, in MeCN solution, shows bands in the terminal CO stretching region at 2 019w, 1 974s, 1 984vs, and 1 887m cm^{-1} and in the

bridging CO stretching region at 1 777m and 1 736m cm^{-1} , in keeping with the solid-state structure (see below).

The dianion can be also obtained by refluxing a mixture of $[\text{NEt}_4][\text{FeH}(\text{CO})_4]$ and $[\text{Ir}_4(\text{CO})_{12}]$ in MeCN, in the molar ratio 4:1. After about 16 h all the starting materials have reacted and impure $[\text{Fe}_2\text{Ir}_2(\text{CO})_{12}]^{2-}$ is formed. This type of preparation, although not selective, is very useful since tetra-alkylammonium salts of the cluster can be obtained, whereas $[\text{Ir}(\text{CO})_4]^-$ or $[\text{Ir}(\text{CO})_2\text{Cl}_2]^-$ are easily available only as salts of very bulky cations, such as $[\text{PPh}_4]^+$ or $[\text{N}(\text{PPh}_3)_2]^+$. The reaction of $\text{Na}_2[\text{Fe}(\text{CO})_4]$ and $[\text{Ir}_4(\text{CO})_{12}]$ was also tested in order to obtain the sodium salt of (2), but this condensation seems to be much less reproducible, and mixtures of products are always obtained. Nevertheless $[\text{Fe}_2\text{Ir}_2(\text{CO})_{12}]^{2-}$ was frequently isolated among the clusters obtained. A large number of different crystals of (2) with different cations such as $[\text{NMe}_3(\text{CH}_2\text{Ph})]^+$, $[\text{PPh}_4]^+$, $[\text{AsPh}_4]^+$, $[\text{NMe}_4]^+$, and $[\text{N}(\text{PPh}_3)_2]^+$ was unsuccessfully tested for X-ray analysis and in all cases the solid-state structures of these derivatives were affected by disorder. Eventually the salt containing the $[\text{NEt}_4]^+$ cation gave crystals of reasonably good quality for data collection and some structural information was obtained (see below). Complex (2) is only moderately soluble in MeOH, thf, and CH_2Cl_2 , very well soluble in MeCN and acetone. The dianion is also stable under a carbon monoxide atmosphere, and, after 24 h of standing in solution at 1 atm CO, no traces of decomposition were detected. Anion (2) can easily be protonated by H_3PO_4 in acetone, yielding quantitatively the monohydridic derivative $[\text{Fe}_2\text{Ir}_2\text{H}(\text{CO})_{12}]^-$ (4). The i.r. spectrum of $[\text{Fe}_2\text{Ir}_2\text{H}(\text{CO})_{12}]^-$ is almost identical in pattern to that of the parent dianion but the absorption bands are shifted to higher wavenumbers [$\nu(\text{CO})$, thf solution, at 2 060w, 2 028s, 2 008vs, 1 998vs, 1 981s, 1 943m, 1 837m, 1 816m, and 1 794w cm^{-1}]. The salts of complex (4) with different bulky cations are also much more soluble than the corresponding salts of the dianion in thf and CH_2Cl_2 . The ^1H n.m.r. spectrum of $[\text{Fe}_2\text{Ir}_2\text{H}(\text{CO})_{12}]^-$ shows, at room temperature, a sharp singlet at $\delta -21.2$. However, on decreasing the temperature the signal broadens and, at 213 K, two signals appear at $\delta -21.7$ and at -19.8 . At 180 K the two signals integrate with a 2.5:1 ratio, suggesting the presence of two different isomers. The value of $\delta -21.16$, calculated from the chemical shifts of the low-temperature spectrum, is in good agreement with the experimental value of $\delta -21.2$ obtained at room temperature. The i.r. spectrum of (4) and the well known isolobality⁶ of the $[\text{Au}(\text{PPh}_3)]^+$ cation with H^+ (see below) indirectly suggest face-bridging co-ordination of the hydrido ligand in one of the isomers of $[\text{Fe}_2\text{Ir}_2\text{H}(\text{CO})_{12}]^-$, but it is difficult to predict the composition of this face. In the other isomer, the hydride can be either bridging a different face or, more probably, edge bridges between one metal of the basal plane and the apical atom. Both locations are very common in tetrahedral hydrido carbonyl clusters.⁷ The existence of different isomers was detected in a series of similar hydrido carbonyl clusters, where the position of the hydrides could be determined by n.m.r. spectroscopy without uncertainty from the ^1H - ^{103}Rh coupling.⁸ The dihydride $[\text{Fe}_2\text{Ir}_2\text{H}_2(\text{CO})_{12}]^{2-}$ derivative can probably be obtained by adding an excess of $\text{CF}_3\text{CO}_2\text{H}$ [$\nu(\text{CO})$ 2 115vw, 2 088m, 2 056s, 2 011m, and 1 978mw, cm^{-1} , toluene solution]; however this compound could not be well characterized since it is not very stable.

The adduct $[\text{Fe}_2\text{Ir}_2(\text{CO})_{12}\{\mu_3\text{-Au}(\text{PPh}_3)\}]^-$ (3) was also prepared. Treatment of an acetone solution of the $[\text{PPh}_4]^+$ salt of the dianion (2) with the stoichiometric amount of $[\text{Au}(\text{PPh}_3)\text{Cl}]$, at room temperature, resulted in an instantaneous colour change from red to brown; i.r. spectroscopy showed the complete disappearance of the starting material; no CO evolution was observed. The i.r. spectrum, shown in Figure 1(c), of the pentanuclear cluster, in thf solution, shows many bands in the

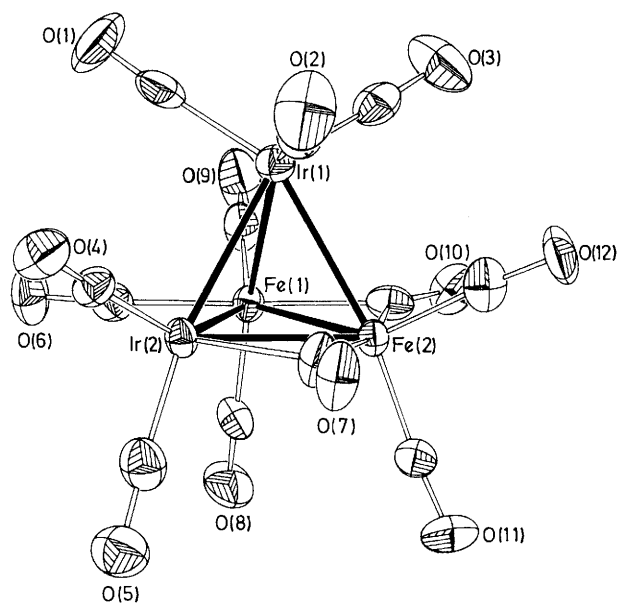


Figure 3. ORTEP drawing of the dianion $[\text{Fe}_2\text{Ir}_2(\text{CO})_{12}]^{2-}$ (2)

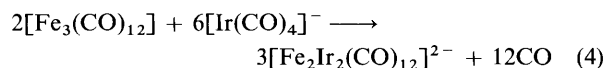
Table 2. Selected distances (Å) and angles (°) in the dianion $[\text{Fe}_2\text{Ir}_2(\text{CO})_{12}]^{2-}$ (2) with e.s.d.s on the last figure in parentheses

M-M		M-CO _b -M	
Ir(1)-Ir(2)	2.734(1)	Ir(2)-C(6)-Fe(1)	81.3(5)
Ir(1)-Fe(1)	2.706(1)	Ir(2)-C(7)-Fe(2)	81.6(5)
Ir(1)-Fe(2)	2.693(2)	Fe(1)-C(10)-Fe(2)	82.5(6)
Ir(2)-Fe(1)	2.685(1)		
Ir(2)-Fe(2)	2.647(2)	M-C-O _b	
Fe(1)-Fe(2)	2.581(2)	Ir(2)-C(6)-O(6)	134(1)
		Ir(2)-C(7)-O(7)	134(1)
M-CO ^{a,b}		Fe(1)-C(6)-O(6)	145(1)
Ir-CO _t	1.863	Fe(1)-C(10)-O(10)	139(1)
Fe-CO _t	1.722	Fe(2)-C(7)-O(7)	144(1)
Ir-CO _b	2.142	Fe(2)-C(10)-O(10)	139(1)
Fe-CO _b	1.947		
C-O _t			
Fe _{bonded}	1.142		
Ir _{bonded}	1.147		
C-O _b	1.183		

^a b = Bridging, t = terminal. ^b Average values.

CO stretching region at 2032m, 1990s, 1977vs, 1964vs, 1945m, 1921w, 1824w, and 1809w cm^{-1} .

The preparation of $[\text{Fe}_2\text{Ir}_2(\text{CO})_{12}]^{2-}$ was also attempted from $[\text{Fe}_3(\text{CO})_{12}]$ and $[\text{Ir}(\text{CO})_4]^-$ according to the formal equation (4). At first a deep red solution was observed which



slowly evolved to a final red-brown solution from which only complex (2) can be isolated. Reaction of $[\text{Fe}_3(\text{CO})_{12}]$ and $[\text{Ir}(\text{CO})_4]^-$ in a 1:1 molar ratio gives a red solution which is stable after 30 min with i.r. bands in the $\nu(\text{CO})$ stretching region at 2020s, 1990vs, 1959m, 1820w, and 1805w cm^{-1} (thf solution). The same product was also obtained from the reaction of $[\text{Ir}(\text{CO})_4]^-$ with an excess of $[\text{Fe}(\text{CO})_5]$ at 60 °C in thf. Any attempt to isolate the red complex failed since, by

precipitation, it is always transformed into the much less soluble $[\text{Fe}_2\text{Ir}_2(\text{CO})_{12}]^{2-}$. However, the stoichiometry (4) and the reproducibility of the i.r. spectrum with a pattern that cannot be explained in terms of a mixture of known homometallic carbonyl clusters of iron or iridium strongly suggests the formulation $[\text{Fe}_3\text{Ir}(\text{CO})_{13}]^-$, analogous to the already reported $[\text{CoFe}_3(\text{CO})_{13}]^-$ and $[\text{CoRu}_3(\text{CO})_{13}]^-$.¹⁰

Crystal Structure of $[\text{N}(\text{PPh}_3)_2][\text{FeIr}_3(\text{CO})_{12}]$ (1).—The solid state structure of complex (1), determined by X-ray single-crystal diffraction techniques, consists of a packing of discrete cations and anions in the molar ratio 1:1 with normal van der Waals contacts between atoms of different ionic fragments. Compound (1) is isomorphous and isostructural with the related salt of $[\text{RuIr}_3(\text{CO})_{12}]^-$.³ A molecular plot of the anion $[\text{FeIr}_3(\mu\text{-CO})_3(\text{CO})_9]^-$ (1) is represented in Figure 2, together with the atom labelling scheme; selected bond distances and angles are listed in Table 1.

The metal skeleton of $[\text{FeIr}_3(\text{CO})_{12}]^-$ consists of a tetrahedral arrangement of metal atoms surrounded by twelve carbonyl groups. Following the nomenclature usually adopted for tetrahedral metal clusters, which adopt the overall stereochemistry of $[\text{Co}_4(\text{CO})_{12}]$ and $[\text{Rh}_4(\text{CO})_{12}]$,¹¹ three carbonyl ligands bridge the edges of the basal face formed by one iron and two iridium atoms; all these metals carry one axial and one radial terminal carbon monoxide group, the remaining three carbonyl groups being bonded to the apical Ir(3). The carbonyl group C(10) is symmetrical whereas the two bridging ligands linking Fe and Ir are markedly asymmetric with short distances towards the Fe atom (average Ir-C 2.20, Fe-C 1.89 Å). This shortening may be a consequence of the distribution of the charge in the cluster: a simple electron counting suggests a formal iron(-1) atom. Thus, a higher tendency to back donation should reduce the M-C bond and elongate the corresponding C-O distances, as observed also for the terminal carbonyl groups. In addition the d^8 metal can be considered, in this compound, as electron deficient and, therefore, more ligand demanding. The same feature has been observed in $[\text{RuIr}_3(\text{CO})_{12}]^-$ and explained in the same terms.³ All the terminal carbon monoxide groups are almost linear, with M-C-O angles ranging from 175 to 178°.

Within the metal framework, the Ir-Ir bond distances range from 2.676(1) to 2.711(1) Å with a mean of 2.696 Å which compares very well with the means of 2.693 and 2.715 Å found in $[\text{Ir}_4(\text{CO})_{12}]$ ¹² and $[\text{RuIr}_3(\text{CO})_{12}]^-$,³ respectively. The Fe-Ir interactions are in the range 2.673(1)–2.691(1) Å with a mean of 2.682 Å. The metal-metal distances in compound (1) can be compared also with those found in $[\text{Fe}_2\text{Ir}_3(\text{CO})_{14}]^-$,¹ which possesses 72 cluster valence electrons (c.v.e.s) (Fe-Ir 2.648, Ir-Ir 2.708 Å) but they are much shorter than the corresponding values found in the elongated trigonal bipyramid $[\text{FeIr}_4(\text{CO})_{15}]^-$ which possesses 76 c.v.e.s (Fe-Ir 2.943, Ir-Ir 2.849 Å).¹

Crystal Structure of $[\text{NET}_4]_2[\text{Fe}_2\text{Ir}_2(\text{CO})_{12}]$ (2).—Crystals of (2) contain discrete molecules of the bulky cations $[\text{NET}_4]^+$ and of the anion $[\text{Fe}_2\text{Ir}_2(\text{CO})_{12}]^{2-}$ in the ratio 2:1. An ORTEP drawing of the anion is reported in Figure 3 which also gives the atom numbering scheme. Selected bond distances and angles are in Table 2.

The tetrahedral metal framework of the cluster, in the solid state, is slightly affected by disorder. The disorder model consists of two tetrahedra with relative occupancy factors of ca. 0.9 and 0.1 with one common vertex, Ir(1), and the opposite face, formed by atoms Ir(2), Fe(1), and Fe(2), rotated by ca. 60°. Nevertheless the carbonyl groups of the moiety with the higher occupancy factor are defined and their stereochemistry well established, resembling that of $[\text{FeIr}_3(\text{CO})_{12}]^-$. Such a different

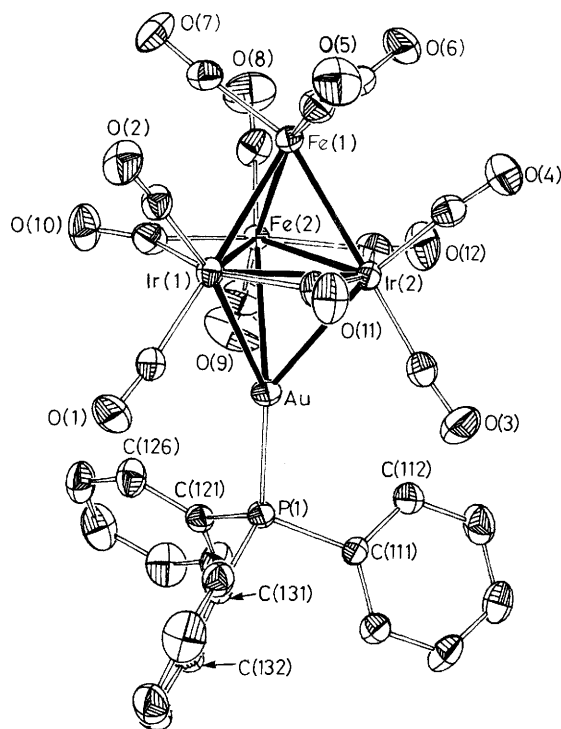


Figure 4. ORTEP drawing of the anion $[\text{Fe}_2\text{Ir}_2(\text{CO})_{12}\{\mu_3\text{-Au}(\text{PPh}_3)\}]^-$ (3)

orientation of the metal cage within an almost perfectly symmetrical icosahedral distribution of the ligands is very common in this kind of compound.¹¹ Within the tetrahedron with occupancy factor of about 0.9 a certain degree of substitutional disorder is observed concerning the Ir(2) and Fe(1) positions so that the iron position is partially occupied by iridium and *vice versa* (see Experimental Section). The refined occupancy factors are in agreement with the postulated 'Fe₂Ir₂' cluster. As a result, an ambiguous pattern of M–M and M–C–O distances arises, and probably a detailed discussion of the molecular parameters of this structure would be meaningless.

Nine carbonyl ligands are linearly bonded to the metals, three to the apical iridium and two to each metal of the basal triangle, with M–C–O angles in the range 173–177°. The Ir–Ir distance 2.734 Å is marginally longer than that found in compounds (1), $[\text{Ir}_4(\text{CO})_{12}]$,¹² and $[\text{RuIr}_3(\text{CO})_{12}]^-$,³ while the average Fe–Ir distance of 2.683 Å compares very well with the average found in derivative (1). Examination of the structures of the tetrahedral clusters $[\text{FeIr}_3(\text{CO})_{12}]^-$ and $[\text{Fe}_2\text{Ir}_2(\text{CO})_{12}]^{2-}$, which contain twelve carbonyl ligands with pseudo C_{3v} type structure, reveals an icosahedral envelope of ligands. On the contrary, in $[\text{Ir}_4(\text{CO})_{12}]$, with T_d symmetry,¹² all the ligands are terminally bonded and define a cubo-octahedral polyhedron. However, the type of environment in (1) and (2) is also present in most substituted Ir₄ clusters,⁷ and represents the best way to pack twelve ligands.¹³

Crystal Structure of $[\text{PPh}_4][\text{Fe}_2\text{Ir}_2(\text{CO})_{12}\{\mu_3\text{-Au}(\text{PPh}_3)\}]^-$ (3).—The crystal structure of (3) consists of $[\text{PPh}_4]^+$ cations and $[\text{Fe}_2\text{Ir}_2(\text{CO})_{12}\{\mu_3\text{-Au}(\text{PPh}_3)\}]^-$ anions with normal Van der Waals contact distances between the cations and the anions. An ORTEP view of the $[\text{Fe}_2\text{Ir}_2(\text{CO})_9(\mu\text{-CO})_3\{\mu_3\text{-Au}(\text{PPh}_3)\}]^-$ anion is presented in Figure 4 together with the atom numbering scheme. Selected bond distances and angles are listed in Table 3.

The polymetallic core is best described as a trigonal-bipyramidal array of metal atoms. The Ir₂Fe basal triangle is

Table 3. Selected distances (Å) and angles (°) in the anion $[\text{Fe}_2\text{Ir}_2(\text{CO})_{12}\{\mu_3\text{-Au}(\text{PPh}_3)\}]^-$ (3) with e.s.d.s on the last figure in parentheses

M–M		M–CO ^{a,b}	
Ir(1)–Ir(2)	2.758(1)	Ir–CO _t	1.845
Ir(1)–Fe(1)	2.686(1)	Fe–CO _t	1.776
Ir(1)–Fe(2)	2.735(1)	Ir–CO _b	2.113
Ir(1)–Au	2.797(1)	Fe–CO _b	1.996
Ir(2)–Fe(1)	2.672(1)		
Ir(2)–Fe(2)	2.776(1)	C–O _t	
Ir(2)–Au	2.829(1)	Fe _{bonded}	1.146
Fe(1)–Fe(2)	2.645(1)	Ir _{bonded}	1.350
Fe(2)–Au	2.806(1)		
		C–O _b	1.166
M–M–M		M–CO _b –M	
Ir(1)–Au–Fe(2)	58.44(1)	Ir(1)–C(10)–Fe(2)	82.2(3)
Ir(1)–Au–Ir(2)	58.70(1)	Ir(1)–C(11)–Ir(2)	83.2(3)
Ir(2)–Au–Fe(2)	59.02(1)	Fe(2)–C(12)–Ir(2)	84.2(3)
Ir(1)–Fe(1)–Fe(2)	61.74(2)		
Ir(1)–Fe(1)–Ir(2)	61.96(2)	M–C _b –O	
Ir(2)–Fe(1)–Fe(2)	62.94(2)	Ir(1)–C(10)–O(10)	133.2(6)
Au–Ir(1)–Fe(2)	60.90(1)	Ir(1)–C(11)–O(11)	135.2(6)
Au–Fe(2)–Ir(1)	60.62(1)	Ir(2)–C(11)–O(11)	141.6(6)
Au–Fe(2)–Ir(2)	60.91(1)	Ir(2)–C(12)–O(12)	135.6(8)
Au–Ir(2)–Fe(2)	60.07(1)	Fe(2)–C(10)–O(10)	144.6(6)
Au–Ir(2)–Ir(1)	60.07(1)	Fe(2)–C(12)–O(12)	140.2(8)
Au–Ir(1)–Ir(2)	61.23(1)		
Fe(1)–Ir(1)–Fe(2)	58.40(2)		
Fe(1)–Fe(2)–Ir(1)	59.87(2)		
Fe(1)–Fe(2)–Ir(2)	59.01(2)		
Fe(1)–Ir(2)–Fe(2)	58.05(2)		
Fe(1)–Ir(2)–Ir(1)	59.26(2)		
Fe(1)–Ir(1)–Ir(2)	58.78(2)		

^a b = Bridging, t = terminal. ^b Average values.

capped on one side by a Fe atom and on the other by a Au(PPh₃) moiety. The apical iron atom bears three terminal CO ligands while the three metals of the equatorial plane bear two terminal and one edge-bridging carbonyl group. The most remarkable change between the structures of $[\text{Fe}_2\text{Ir}_2(\text{CO})_{12}]^{2-}$ and $[\text{Fe}_2\text{Ir}_2(\text{CO})_{12}\{\text{Au}(\text{PPh}_3)\}]^-$ is that in compound (2) the apical atom is iridium while in compound (3) it is iron. A possible explanation of this interchange arises from the tendency to maximize the metal–metal interactions between heavier elements and from the well known fluxionality of the carbon monoxide groups which in (3) arrange to leave room for the bulky Au(PPh₃) group.^{14,15} As a result, in (3) is present an isomeric form of complex (2) with an unchanged metal cage rotated within an unchanged ligand envelop. The PPh₃ ligand is bound to gold with a Au–P(1) distance of 2.279(2) Å equal to the value of 2.279(8) Å found in $[\text{Au}(\text{PPh}_3)\text{Me}]$ ¹⁶ where the Au^I is *sp* hybridized; also in compound (3) we can consider the lobe of the *sp* hybrid pointing towards the centre of the Ir₂Fe triangle. The geometry around the gold atom indicates the *sp* hybridization {P–Au–midpoint [Ir(1)–Ir(2)–Fe(2) triangle] 173°}. With regard to the three bridging carbonyls only C(10) is markedly asymmetric with a short distance toward Fe(2) [Ir(1)–C(10) 2.20(1), Fe(2)–C(10) 1.95(1) Å]; the M–C distances of the other μ-CO ligands are: Ir(2)–C(12) 2.10(1), Fe(2)–C(12) 2.04(1); Ir(1)–C(11) 2.13(1); and Ir(2)–C(11) 2.02 Å. No significant deviation from linearity has been found for the terminal CO groups with the M–C–O angles ranging from 172 to 178°. In the equatorial triangle two positions, denoted Ir(2) and Fe(2), are affected by positional disorder (see Experimental Section) to such an extent that the molecular parameters of the portion 'Fe₂Ir₂' cannot be discussed in detail. However, the M–Au edges are in the range 2.797(1)–2.829(1) Å, with an average separation

of 2.813 Å which is in good agreement with the sum of metallic radii.¹⁷ The shortest M–M bonds are the unbridged Fe(1)–M distances (average 2.679 Å); the average M–M bond distance in the equatorial plane is 2.756 Å.

A simple electron counting shows that, if we consider $[\text{Au}(\text{PPh}_3)]^+$ as a ligand and therefore acting as a one-electron donor to the tetrahedral cluster (isolobal analogy),⁶ compound (3) is electron precise possessing 60 c.v.e.s, whereas considering the gold atom as a part of the whole cluster there are 72 c.v.e.s in agreement with electron-counting rules which predict this value for a trigonal bipyramid.¹⁸

Experimental

All reactions were carried out under an atmosphere of nitrogen or carbon monoxide with Schlenk-tube and vacuum-line techniques.¹⁹ Solvents were purified and dried by distillation under a nitrogen atmosphere from the following solvent/drier combinations: thf/sodium diphenylketyl; methanol/Mg; $\text{CH}_2\text{Cl}_2/\text{P}_2\text{O}_5$; $\text{Pr}^i\text{OH}/\text{Al}(\text{OPr}^i)$.³

Infrared spectra were recorded on a Perkin-Elmer 781 grating spectrophotometer using calcium fluoride cells previously purged with nitrogen or carbon monoxide. N.m.r. spectra were recorded on a Bruker AC 200 spectrometer and are reported downfield of the internal standard SiMe_4 . Fast atom bombardment mass spectra (f.a.b. m.s.) were recorded on a V.G. 7070EQ mass spectrometer equipped with an H.F. magnet and a standard f.a.b. source with xenon gas at 8 keV (1.28×10^{-15} J) (3-nitrobenzyl alcohol with 10% tetrahydrothiophene 1,1-dioxide). The isotopic patterns were simulated for all compounds and are in excellent agreement with the experimental spectra.

The compounds $[\text{Ir}_4(\text{CO})_{12}]$,²⁰ $[\text{N}(\text{PPh}_3)_2][\text{Ir}(\text{CO})_2\text{Cl}_2]$,²¹ $[\text{Fe}_2(\text{CO})_9]$,²² $[\text{Au}(\text{PPh}_3)\text{Cl}]$,²³ $[\text{N}(\text{PPh}_3)_2][\text{Ir}(\text{CO})_4]$,²⁴ $[\text{NEt}_4][\text{FeH}(\text{CO})_4]$,²⁵ $[\text{N}(\text{PPh}_3)_2]_2[\text{FeIr}_4(\text{CO})_{15}]$,¹ and $\text{Na}_2[\text{Fe}(\text{CO})_4]$ ²⁶ were prepared as described.

Preparations.— $[\text{N}(\text{PPh}_3)_2][\text{FeIr}_3(\text{CO})_{12}]$ (1). (a) The compounds $[\text{Ir}_4(\text{CO})_{12}]$ (0.839 g, 0.76 mmol) and $[\text{Fe}(\text{CO})_5]$ (0.114 cm³, 0.84 mmol) were suspended in MeOH (30 cm³). The vessel was evacuated and filled with carbon monoxide. To this suspension NaOH (1.14 g, 28.5 mmol) was added and the mixture stirred, at room temperature, for 6 h during which time the colour of the solution changed from canary-yellow to orange-yellow and the i.r. spectrum showed complete transformation of the starting materials into $[\text{FeIr}_4(\text{CO})_{15}]^{2-}$. The solution was stirred for 5 d whereupon complete transformation of the pentanuclear cluster into $[\text{FeIr}_3(\text{CO})_{12}]^-$ and $[\text{Ir}(\text{CO})_4]^-$ occurred. The solution was filtered and the residue washed with MeOH (2×5 cm³) and $[\text{N}(\text{PPh}_3)_2]\text{Cl}$ (0.96 g, 1.67 mmol) was added to the filtrate. The MeOH was removed under vacuum and the residue dissolved in thf (50 cm³). This solution was filtered and treated with 2-propanol (50 cm³) and the solvent was removed *in vacuo*. When the volume of the solution was about 40 cm³ an ivory precipitate, mainly $[\text{N}(\text{PPh}_3)_2][\text{Ir}(\text{CO})_4]$, was formed which was collected by filtration, washed with 2-propanol (2×5 cm³), and vacuum dried (0.309 g). The 2-propanol–thf mother-liquor was reduced in volume *in vacuo* and when the volume was about 20 cm³ an orange precipitate was formed which was collected by filtration, washed with 2-propanol (2×5 cm³), and dried *in vacuo*, $[\text{N}(\text{PPh}_3)_2][\text{FeIr}_3(\text{CO})_{12}]$, yield 0.607 g (53%) (Found: C, 38.1; H, 2.0; N, 0.9. Calc. for $\text{C}_{48}\text{H}_{30}\text{FeIr}_3\text{NO}_{12}\text{P}_2$: C, 38.2; H, 2.0; N, 0.9%).

(b) The salt $[\text{N}(\text{PPh}_3)_2]_2[\text{FeIr}_4(\text{CO})_{15}] \cdot 2\text{C}_4\text{H}_8\text{O}$ (0.735 g, 0.298 mmol) was dissolved in thf (15 cm³) and the Schlenk tube was evacuated and refilled with carbon monoxide. The solution was stirred, at room temperature, for 4 d whereupon complete transformation into $[\text{Ir}(\text{CO})_4]^-$ and $[\text{FeIr}_3(\text{CO})_{12}]^-$ occurred.

Anion (1) was isolated as described above, $[\text{N}(\text{PPh}_3)_2][\text{Ir}(\text{CO})_4]$ (0.123 g); $[\text{N}(\text{PPh}_3)_2][\text{FeIr}_3(\text{CO})_{12}]$, yield 0.274 g (61%) f.a.b. m.s. (negative ions): m/z (⁵⁶Fe, ¹⁹³Ir) 971 $[M - \text{N}(\text{PPh}_3)_2]$ and $971 - 28x$ $[\text{FeIr}_3(\text{CO})_{12-x}]^-$ ($x = 1-7$).

$[\text{N}(\text{PPh}_3)_2]_2[\text{Fe}_2\text{Ir}_2(\text{CO})_{12}]$ (2). (a) In a Schlenk tube, equipped with a cold finger, were placed $[\text{Fe}_2(\text{CO})_9]$ (0.030 g, 0.08 mmol), $[\text{N}(\text{PPh}_3)_2][\text{Ir}(\text{CO})_4]$ (0.098 g, 0.10 mmol), and acetone (10 cm³). The mixture was refluxed for 3 h and checked by i.r. spectroscopy which showed some unreacted $[\text{Ir}(\text{CO})_4]^-$. Small portions of $[\text{Fe}_2(\text{CO})_9]$ were added until all the $[\text{Ir}(\text{CO})_4]^-$ had reacted. The solvent was evacuated, the brown solid washed with MeOH (10 cm³), and the residue dissolved with acetone (4 cm³) and crystallized by layering of 2-propanol (15 cm³). Yield 0.071 g (64%) (Found: C, 50.3; H, 3.1; N, 1.3. Calc. for $\text{C}_{84}\text{H}_{60}\text{Fe}_2\text{Ir}_2\text{N}_2\text{O}_{12}\text{P}_4$: C, 52.8; H, 3.2; N, 1.5%). F.a.b. m.s. (negative ions): m/z (⁵⁶Fe, ¹⁹³Ir) 1372 $[M - \text{N}(\text{PPh}_3)_2]$, 834 $[M - 2\text{N}(\text{PPh}_3)_2]$, and $834 - 28x$ $[\text{Fe}_2\text{Ir}_2(\text{CO})_{12-x}]^-$ ($x = 1-10$).

(b) In a round-bottomed flask (100 cm³) were placed $[\text{PPh}_4][\text{Ir}(\text{CO})_2\text{Cl}_2]$ (0.21 g, 0.32 mmol), $[\text{NEt}_4][\text{FeH}(\text{CO})_4]$ (0.29 g, 0.97 mmol), and thf (20 cm³). The mixture was stirred at room temperature for 5 d. The solvent was then removed *in vacuo*, and the dark residue suspended in MeOH (15 cm³). Solid $[\text{PPh}_4]\text{Br}$ (0.2 g) was added and the mixture stirred for 3 h. The microcrystalline solid was collected by filtration, washed with MeOH (2×5 cm³), and crystallized from acetone–2-propanol. Yield 0.216 g (90%).

(c) In a Schlenk tube, equipped with a cold finger, we placed $[\text{Ir}_4(\text{CO})_{12}]$ (0.27 g, 0.24 mmol), $[\text{NEt}_4][\text{FeH}(\text{CO})_4]$ (0.29 g, 0.97 mmol), and MeCN (10 cm³). The mixture was refluxed for 16 h then the solvent was removed *in vacuo*. The brown residue was suspended in MeOH (20 cm³) and solid $[\text{NEt}_4]\text{Cl}$ (0.3 g) added. The suspension was stirred for 2 h, and the microcrystalline precipitate collected by filtration, washed with MeOH (3×5 cm³), and dried. The crude product was dissolved in acetone (6 cm³) and crystallized by layering of 2-propanol (15 cm³). Yield 0.285 g (54%) (Found: C, 30.6; H, 3.5; Fe, 11.4; Ir, 34.0; N, 2.4. Calc. for $\text{C}_{28}\text{H}_{40}\text{Fe}_2\text{Ir}_2\text{N}_2\text{O}_{12}$: C, 30.8; H, 3.7; Fe, 10.2; Ir, 35.2; N, 2.6%).

$[\text{PPh}_4][\text{Fe}_2\text{Ir}_2(\text{CO})_{12}\{\mu_3\text{-Au}(\text{PPh}_3)\}]$ (3). The salt $[\text{PPh}_4]_2[\text{Fe}_2\text{Ir}_2(\text{CO})_{12}]$ (0.216 g, 0.143 mmol) was dissolved in acetone (10 cm³). Solid $[\text{Au}(\text{PPh}_3)\text{Cl}]$ (0.078 g, 0.16 mmol) was added and the solution immediately changed colour. After 1 h of stirring the solvent was evacuated and the crude residue suspended in 2-propanol. The mixture was stirred for 1 h, and the colourless solvent is collected by syringe. The dark solid was dried *in vacuo* and crystallized from thf–cyclohexane. Yield 0.216 g (93%) (Found: C, 40.4; H, 2.1. Calc. for $\text{C}_{54}\text{H}_{35}\text{AuFe}_2\text{Ir}_2\text{O}_{12}\text{P}_2$: C, 39.8; H, 2.2%). F.a.b. m.s. (negative ions): m/z (⁵⁶Fe, ¹⁹³Ir, ¹⁹⁷Au) 1291 $[M - \text{PPh}_4]$ and $1291 - 28x$ $[\text{Fe}_2\text{Ir}_2(\text{CO})_{12-x}\text{Au}(\text{PPh}_3)]^-$ ($x = 1-8$).

Collection and Reduction of the X-Ray Data for Complexes (1)–(3).—The crystal data for compounds (1)–(3) are summarized in Table 4 together with some experimental details. Crystals of the three compounds were mounted in an arbitrary orientation on a glass fibre which was then fixed into an aluminium pin and mounted onto a goniometer head. Diffraction data were collected on an Enraf–Nonius CAD4 automated diffractometer, controlled by a PDP 11/73 computer, using Mo-K_α radiation ($\lambda = 0.71073$ Å) with a graphite crystal monochromator in the incident beam. The Enraf–Nonius program SEARCH was employed to obtain 25 accurately centred reflections which were then used in the program INDEX to obtain an orientation matrix for data collection and to provide cell dimensions.²⁷ A periodic remeasurement of three standard reflections revealed a crystal decay, on X-ray exposure, which was evaluated as about 15% for (1), 7% for (2), and 10% for (3).

Table 4. Summary of crystal data and intensity collection parameters for compounds (1)–(3)^a

Compound	[N(PPh ₃) ₂][FeIr ₃ (CO) ₁₂]	[NEt ₄] ₂ [Fe ₂ Ir ₂ (CO) ₁₂]	[PPh ₄][Fe ₂ Ir ₂ (CO) ₁₂ {μ ₃ -Au(PPh ₃) ₃ }
Formula	C ₄₈ H ₃₀ FeIr ₃ NO ₁₂ P ₂	C ₂₈ H ₄₀ Fe ₂ Ir ₂ N ₂ O ₁₂	C ₅₄ H ₃₅ AuFe ₂ Ir ₂ O ₁₂ P ₂
<i>M</i>	1 507.17	1 092.73	1 630.88
Space group	<i>P</i> 2 ₁ / <i>c</i>	<i>P</i> 2 ₁	<i>P</i> 2 ₁ / <i>c</i>
<i>a</i> /Å	14.968(2)	9.072(5)	10.990(3)
<i>b</i> /Å	19.892(2)	19.910(5)	13.693(2)
<i>c</i> /Å	16.610(2)	10.094(3)	35.883(3)
β/°	96.10(2)	91.92(3)	97.39(2)
<i>U</i> /Å ³	4 917(2)	1 822(2)	5 355(3)
<i>Z</i>	4	2	4
<i>D_c</i> /g cm ⁻³	2.036	1.991	2.023
μ(Mo-Kα)/cm ⁻¹	84.75	80.90	83.06
ω-scan width/°	1.20 + 0.35tanθ	1.20 + 0.35tanθ	1.80 + 0.35tanθ
Measured reflections	8 649	3 291	9 571
Unique observed reflections	5 065	2 602	6 666
[<i>I</i> > 3σ(<i>I</i>)]			
Final <i>R</i> , <i>R</i> ' ^b	0.032, 0.040	0.033, 0.040	0.031, 0.040
No. of variables	419	336	538
Min. transmission factor	0.65	0.63	0.56
E.s.d. ^c	1.115	1.392	1.404

^a Details common to all three compounds: monoclinic; scan mode, ω, θ range 3–25°; octants in reciprocal space explored, ±*h*, +*k*, +*l*. ^b *R* = [Σ(*F_o* - *k*|*F_c*|)/Σ*F_o*], *R*' = [Σ*w*(*F_o* - *k*|*F_c*|)²/Σ*wF_o*²]^{1/2}. ^c [Σ*w*(*F_o* - *k*|*F_c*|)²/(*N_o* - *N_v*)]^{1/2} where *N_o* = number of observations and *N_v* = number of variables.

Table 5. Fractional atomic co-ordinates for complex (1) with e.s.d.s in parentheses

Atom	<i>x</i>	<i>y</i>	<i>z</i>	Atom	<i>x</i>	<i>y</i>	<i>z</i>
Ir(1)	0.144 71(3)	0.029 81(2)	-0.036 21(2)	C(114)	0.489 0(8)	-0.091 9(6)	-0.306 0(7)
Ir(2)	0.217 94(3)	0.142 01(2)	0.030 80(3)	C(115)	0.404 2(8)	-0.097 8(6)	-0.279 2(7)
Ir(3)	0.309 97(3)	0.024 53(2)	0.046 38(2)	C(116)	0.328 8(7)	-0.082 9(5)	-0.333 5(6)
Fe	0.284 59(8)	0.086 23(6)	-0.097 76(7)	C(121)	0.147 0(6)	-0.039 0(5)	-0.430 3(6)
P(1)	0.244 3(2)	-0.046 1(1)	-0.484 0(1)	C(122)	0.142 0(8)	0.013 8(6)	-0.374 3(7)
P(2)	0.261 9(2)	-0.174 8(1)	-0.567 3(1)	C(123)	0.068 9(8)	0.016 2(6)	-0.330 1(7)
O(1)	-0.014 4(5)	0.076 2(4)	-0.150 3(5)	C(124)	0.003 4(9)	-0.028 7(6)	-0.340 2(8)
O(2)	0.093 5(5)	-0.114 8(3)	-0.014 5(5)	C(125)	0.003 1(9)	-0.078 1(7)	-0.398 3(8)
O(3)	0.090 1(6)	0.250 0(5)	-0.035 3(8)	C(126)	0.076 4(8)	-0.082 8(6)	-0.443 9(7)
O(4)	0.296 3(7)	0.207 0(5)	0.186 1(6)	C(131)	0.262 7(6)	0.033 4(4)	-0.530 4(5)
O(5)	0.214 2(7)	0.158 4(5)	-0.242 3(6)	C(132)	0.237 0(6)	0.043 0(4)	-0.611 8(6)
O(6)	0.457 3(5)	0.053 7(5)	-0.149 5(5)	C(133)	0.244 9(7)	0.103 7(5)	-0.649 0(6)
O(7)	0.350 3(6)	-0.112 1(4)	-0.022 6(5)	C(134)	0.279 5(8)	0.157 6(6)	-0.603 2(8)
O(8)	0.252 5(7)	-0.022 4(5)	0.205 8(5)	C(135)	0.309 3(8)	0.149 4(6)	-0.523 0(7)
O(9)	0.486 5(5)	0.095 7(4)	0.097 9(5)	C(136)	0.299 5(7)	0.087 7(5)	-0.486 6(6)
O(10)	0.077 2(5)	0.074 8(4)	0.125 4(4)	C(211)	0.364 8(6)	-0.174 6(4)	-0.613 3(5)
O(11)	0.228 3(5)	-0.042 6(4)	-0.176 7(4)	C(212)	0.416 6(7)	-0.232 4(5)	-0.620 0(6)
O(12)	0.389 1(5)	0.203 4(3)	-0.032 8(5)	C(213)	0.494 7(7)	-0.229 2(6)	-0.653 7(7)
N	0.228 9(5)	-0.100 5(4)	-0.553 2(4)	C(214)	0.525 6(8)	-0.171 3(6)	-0.683 8(7)
C(1)	0.042 8(7)	0.057 7(5)	-0.105 8(6)	C(215)	0.475 4(8)	-0.113 2(6)	-0.678 8(7)
C(2)	0.109 3(6)	-0.059 7(5)	-0.022 9(6)	C(216)	0.394 8(7)	-0.114 9(5)	-0.644 9(6)
C(3)	0.138 6(8)	0.210 4(6)	-0.010 8(9)	C(221)	0.175 4(6)	-0.215 3(4)	-0.635 4(6)
C(4)	0.266 2(7)	0.183 6(5)	0.125 5(7)	C(222)	0.183 9(7)	-0.282 2(5)	-0.655 8(6)
C(5)	0.241 6(7)	0.130 3(5)	-0.183 9(7)	C(223)	0.114 6(8)	-0.312 2(6)	-0.705 1(7)
C(6)	0.387 9(7)	0.066 4(5)	-0.127 1(6)	C(224)	0.040 7(9)	-0.276 7(7)	-0.733 2(8)
C(7)	0.337 4(7)	-0.061 3(5)	0.003 7(6)	C(225)	0.031 5(9)	-0.210 3(7)	-0.714 6(8)
C(8)	0.271 5(7)	-0.004 0(5)	0.146 7(6)	C(226)	0.102 6(8)	-0.178 9(6)	-0.665 7(7)
C(9)	0.421 4(7)	0.067 3(5)	0.076 9(6)	C(231)	0.279 9(6)	-0.226 2(5)	-0.477 6(6)
C(10)	0.118 1(6)	0.078 8(5)	0.070 2(6)	C(232)	0.364 6(8)	-0.233 5(6)	-0.438 4(7)
C(11)	0.228 7(6)	0.004 9(5)	-0.132 9(6)	C(233)	0.376 0(9)	-0.271 5(7)	-0.364 6(9)
C(12)	0.332 4(7)	0.162 2(5)	-0.040 0(7)	C(234)	0.305 1(1)	-0.298 8(7)	-0.339 8(9)
C(111)	0.339 5(6)	-0.061 7(4)	-0.410 5(5)	C(235)	0.222 5(9)	-0.291 8(7)	-0.372 8(8)
C(112)	0.425 4(7)	-0.054 3(5)	-0.432 7(6)	C(236)	0.207 1(8)	-0.253 9(6)	-0.447 0(7)
C(113)	0.499 4(7)	-0.071 6(5)	-0.382 1(7)				

on *F_o* at the end of data collection. Lorentz, polarization, decay, and absorption corrections were applied, the latter performed with the empirical method described in ref. 28.

Solution and Refinement of the Structures.—The structures were solved by the heavy-atom method: a three-dimensional

Patterson map was used to locate the metal core and Fourier difference syntheses followed by successive least-squares refinements were used to locate the other non-hydrogen atoms. The refinement was carried out by full-matrix least-squares, with anisotropic thermal parameters for all the atoms of the anions and was continued until the largest shift in any parameter was

Table 6. Fractional atomic co-ordinates for complex (2) with e.s.d.s in parentheses

Atom	x	y	z	Atom	x	y	z
Ir(1)	0.322 18(6)	0.001 41(4)	0.156 77(6)	C(5)	-0.038(2)	0.147 9(9)	0.240(2)
Ir(2)	0.109 14(6)	0.097 0	0.187 80(6)	C(6)	-0.007(2)	0.030 1(8)	0.055(1)
Ir(3)	0.070 7(6)	-0.014 8(3)	0.345 1(5)	C(7)	0.237(2)	0.112 5(7)	0.367(1)
Fe(1)	0.040 0(2)	-0.034 22(8)	0.199 8(1)	C(8)	-0.139(1)	-0.028 3(8)	0.260(1)
Fe(2)	0.194 1(2)	0.020 19(9)	0.390 8(2)	C(9)	0.046(2)	-0.107 2(8)	0.114(1)
Fe(3)	0.346(2)	0.026 5(7)	0.278(1)	C(10)	0.135(1)	-0.072 8(7)	0.360(1)
Fe(4)	0.173 4(9)	-0.030 8(5)	0.097 2(8)	C(11)	0.077(2)	0.030 5(8)	0.522(1)
O(1)	0.298(2)	-0.014 6(9)	-0.142(1)	C(12)	0.355(2)	0.000 4(8)	0.483(1)
O(2)	0.566(1)	0.108 1(9)	0.200(1)	C(111)	0.699(2)	-0.080 6(8)	-0.216(1)
O(3)	0.462(1)	-0.127 3(7)	0.248(2)	C(112)	0.674(2)	-0.088(1)	-0.066(2)
O(4)	0.239(1)	0.198 4(6)	0.015(1)	C(121)	0.873(2)	-0.177 0(8)	-0.240(1)
O(5)	-0.137(1)	0.182 8(7)	0.280(1)	C(122)	1.011(2)	-0.134(1)	-0.255(2)
O(6)	-0.071(1)	0.037 6(6)	-0.047(1)	C(131)	0.746(1)	-0.126 7(8)	-0.439(1)
O(7)	0.301(1)	0.159 6(5)	0.415(1)	C(132)	0.778(2)	-0.183 5(9)	-0.527(2)
O(8)	-0.257(1)	-0.034 2(7)	0.294(1)	C(141)	0.612(2)	-0.198 1(8)	-0.274(1)
O(9)	0.041(2)	-0.159 7(7)	0.063(1)	C(142)	0.461(2)	-0.176(1)	-0.320(2)
O(10)	0.147(1)	-0.125 4(6)	0.413(1)	C(211)	0.770(2)	0.223(1)	0.699(2)
O(11)	0.007(1)	0.036 1(8)	0.614(1)	C(212)	0.934(2)	0.202(1)	0.744(2)
O(12)	0.452(1)	-0.013 7(7)	0.548(1)	C(221)	0.668(2)	0.163(1)	0.900(2)
N(1)	0.736(1)	-0.146 4(6)	-0.293(1)	C(222)	0.646(2)	0.229(1)	0.978(2)
N(2)	0.664(1)	0.172 2(6)	0.745(1)	C(231)	0.509(2)	0.197(1)	0.701(2)
C(1)	0.300(2)	-0.009 3(9)	-0.034(2)	C(232)	0.385(2)	0.155(1)	0.732(2)
C(2)	0.477(2)	0.066 7(9)	0.192(2)	C(241)	0.686(2)	0.105(1)	0.688(2)
C(3)	0.404(2)	-0.078 0(9)	0.214(1)	C(242)	0.692(2)	0.105(1)	0.539(2)
C(4)	0.187(1)	0.159 9(7)	0.078(1)				

The atoms labelled Ir(3), Fe(3), and Fe(4) have occupancy factors of *ca.* 0.1 (see text).

Table 7. Fractional atomic co-ordinates for complex (3) with e.s.d.s in parentheses

Atom	x	y	z	Atom	x	y	z
Au	0.140 72(3)	0.409 45(2)	0.655 05(1)	C(121)	-0.055 4(7)	0.470 3(6)	0.718 0(2)
Ir(1)	0.133 70(3)	0.344 79(2)	0.580 87(1)	C(122)	-0.073 7(8)	0.478 6(7)	0.755 0(2)
Ir(2)	0.343 49(3)	0.312 99(3)	0.630 35(1)	C(123)	-0.182 6(9)	0.452 3(9)	0.766 4(3)
Fe(1)	0.257 9(1)	0.175 91(8)	0.580 79(3)	C(124)	-0.275 9(8)	0.416 3(8)	0.741 5(3)
Fe(2)	0.129 76(5)	0.210 03(4)	0.636 96(1)	C(125)	-0.258 9(8)	0.405 5(7)	0.703 9(3)
P(1)	0.082 6(2)	0.512 0(1)	0.699 52(5)	C(126)	-0.148 1(8)	0.432 4(7)	0.692 5(3)
P(2)	0.435 6(2)	0.277 2(2)	0.406 86(6)	C(131)	0.040 5(7)	0.634 0(5)	0.682 8(2)
O(1)	-0.007 7(7)	0.533 2(5)	0.572 4(2)	C(132)	-0.034 0(8)	0.692 5(6)	0.700 9(3)
O(2)	0.089 6(6)	0.306 2(6)	0.498 5(2)	C(133)	-0.067 4(8)	0.784 4(6)	0.687 3(3)
O(3)	0.451 9(7)	0.470 7(6)	0.680 6(2)	C(134)	-0.025(1)	0.818 4(7)	0.655 7(3)
O(4)	0.582 3(6)	0.224 6(5)	0.620 8(2)	C(135)	0.051(1)	0.761 0(8)	0.637 6(3)
O(5)	0.416 1(7)	0.213 3(6)	0.522 9(2)	C(136)	0.084 7(8)	0.670 0(6)	0.650 7(3)
O(6)	0.398 0(7)	0.011 3(5)	0.615 3(2)	C(211)	0.573 7(7)	0.243 9(6)	0.436 5(2)
O(7)	0.074 5(6)	0.060 6(5)	0.533 4(2)	C(212)	0.671 3(9)	0.312 3(7)	0.440 6(3)
O(8)	0.106 7(8)	0.000 4(5)	0.631 5(2)	C(213)	0.781(1)	0.286 6(8)	0.463 1(3)
O(9)	0.003 5(8)	0.223 8(6)	0.703 8(2)	C(214)	0.790(1)	0.199 2(8)	0.480 4(3)
O(10)	-0.107 1(5)	0.229 2(5)	0.586 7(2)	C(215)	0.698(1)	0.132 7(8)	0.476 9(3)
O(11)	0.369 8(5)	0.446 3(5)	0.564 8(2)	C(216)	0.585 5(9)	0.157 5(7)	0.454 6(3)
O(12)	0.346 8(7)	0.171 7(5)	0.696 3(2)	C(221)	0.464 2(7)	0.282 9(6)	0.358 7(2)
C(1)	0.046 0(7)	0.464 0(6)	0.578 0(2)	C(222)	0.365 7(8)	0.305 9(6)	0.331 1(2)
C(2)	0.107 6(8)	0.318 6(7)	0.529 3(2)	C(223)	0.387 0(9)	0.314 4(7)	0.294 1(3)
C(3)	0.403 6(8)	0.410 1(7)	0.662 0(3)	C(224)	0.502 0(9)	0.299 0(7)	0.284 4(3)
C(4)	0.486 5(8)	0.256 1(6)	0.623 1(2)	C(225)	0.597 2(9)	0.274 2(7)	0.311 3(3)
C(5)	0.352 2(8)	0.200 3(7)	0.546 0(2)	C(226)	0.579 4(8)	0.267 1(7)	0.347 8(3)
C(6)	0.345 5(8)	0.075 6(7)	0.601 1(2)	C(231)	0.324 0(7)	0.182 9(6)	0.410 8(2)
C(7)	0.142 7(8)	0.108 0(6)	0.551 2(2)	C(232)	0.235 4(8)	0.194 0(6)	0.435 3(3)
C(8)	0.121 5(8)	0.083 1(6)	0.632 4(3)	C(233)	0.161 8(9)	0.112 9(7)	0.441 3(3)
C(9)	0.052 0(8)	0.224 4(7)	0.677 6(3)	C(234)	0.178 0(9)	0.025 5(7)	0.423 8(3)
C(10)	-0.005 4(8)	0.245 7(6)	0.598 5(3)	C(235)	0.262 5(9)	0.016 1(7)	0.398 9(3)
C(11)	0.317 1(7)	0.396 8(6)	0.583 5(2)	C(236)	0.334 2(8)	0.096 8(6)	0.392 8(3)
C(12)	0.296 6(9)	0.208 8(7)	0.669 1(2)	C(241)	0.383 9(7)	0.394 8(5)	0.421 7(2)
C(111)	0.199 0(6)	0.526 9(5)	0.739 9(2)	C(242)	0.384 6(8)	0.410 7(6)	0.459 9(2)
C(112)	0.273 3(8)	0.447 3(6)	0.751 6(2)	C(243)	0.342 7(9)	0.498 9(7)	0.472 4(3)
C(113)	0.362 0(9)	0.456 4(7)	0.782 2(3)	C(244)	0.306 6(8)	0.570 9(7)	0.447 3(3)
C(114)	0.377 4(8)	0.544 4(7)	0.801 8(2)	C(245)	0.307 8(8)	0.557 1(7)	0.410 1(3)
C(115)	0.303 1(9)	0.620 2(7)	0.790 7(3)	C(246)	0.347 8(8)	0.468 5(6)	0.396 7(2)
C(116)	0.215 7(8)	0.613 2(6)	0.759 8(2)				

less than 0.3σ . All the hydrogen atoms were introduced in the models at calculated positions but not refined. The function minimized was $\sum w(F_o - k|F_c|)^2$. Individual weights were $w = 1/\sigma^2(F_o)$ where $\sigma(F_o) = \sigma(F_o^2)/2F_o$, $\sigma(F_o^2) = [\sigma^2(I) + (pI)^2]^{1/2}/Lp$ and p the 'ignorance factor' was equal to 0.04 for the three compounds. Scattering factors and anomalous dispersion corrections were taken from ref. 29.

The positional parameters for compounds (1)–(3) are listed in Tables 5–7. For (2) the occupancy factors for the atoms Ir(2) and Fe(1) involved in substitutional disorder are 0.83 and 1.23. This corresponds to the metal distributions $\text{Fe}_{0.12}\text{Ir}_{0.88}$ for Ir(2) and $\text{Fe}_{0.88}\text{Ir}_{0.12}$ for Fe(1). For compound (3) the atoms labelled as Ir(2) and Fe(2) showed, in the first stages of the refinement, anomalous thermal parameters. Their occupancy factors refined to final values of 0.75 and 1.75, respectively, which afford the metal distributions $\text{Fe}_{0.62}\text{Ir}_{0.38}$ for the Fe(2) site and $\text{Fe}_{0.38}\text{Ir}_{0.62}$ for the Ir(2) site.

Additional material available from the Cambridge Crystallographic Data Centre comprises H-atom co-ordinates, thermal parameters, and remaining bond lengths and angles.

Acknowledgements

We thank the Italian Consiglio Nazionale delle Ricerche (C. N. R.) for financial support.

References

- Part 1, R. Della Pergola, L. Garlaschelli, F. Demartin, M. Manassero, N. Masciocchi, M. Sansoni, and A. Fumagalli, *J. Chem. Soc., Dalton Trans.*, 1989, 1109.
- R. Della Pergola, F. Demartin, L. Garlaschelli, and M. Manassero, unpublished work.
- A. Fumagalli, F. Demartin, and A. Sironi, *J. Organomet. Chem.*, 1985, **279**, C33.
- A. Fumagalli, T. F. Koetzle, and F. Takusagawa, *J. Organomet. Chem.*, 1981, **213**, 365.
- P. Chini, G. Ciani, L. Garlaschelli, M. Manassero, S. Martinengo, A. Sironi, and F. Canziani, *J. Organomet. Chem.*, 1978, **152**, C35; L. Garlaschelli, S. Martinengo, P. Chini, F. Canziani, and R. Bau, *ibid.*, 1981, **213**, 379; R. Della Pergola, L. Garlaschelli, S. Martinengo, F. Demartin, M. Manassero, and M. Sansoni, *Gazz. Chim. Ital.*, 1987, **117**, 245.
- M. Elia, M. M. L. Chen, D. M. P. Mingos, and R. Hoffmann, *Inorg. Chem.*, 1976, **15**, 1148; R. Hoffmann, *Angew. Chem., Int. Ed. Engl.*, 1982, **21**, 711; K. P. Hall and D. M. P. Mingos, *Prog. Inorg. Chem.*, 1984, **32**, 237; J. W. Lauher and K. Wald, *J. Am. Chem. Soc.*, 1981, **103**, 7648.
- P. R. Raithby, in 'Transition Metal Clusters,' ed. B. F. G. Johnson, Wiley, New York, 1980, p. 5; D. H. Farrar and R. J. Goudsmit, in 'Metal Clusters,' ed. M. Moskovits, Wiley, New York, 1986, p. 29; G. L. Geoffroy, in 'Metal Clusters in Catalysis,' eds. B. C. Gates, L. Gucci, and H. Knozinger, Elsevier, Amsterdam, 1986, p. 21.
- J. Pursiainen and T. A. Pakkanen, *J. Organomet. Chem.*, 1989, **362**, 375.
- P. Chini and B. T. Heaton, *Top. Curr. Chem.*, 1977, **77**, 1; P. C. Steinhardt, W. L. Gladfelter, A. D. Harley, J. R. Fox, and G. L. Geoffroy, *Inorg. Chem.*, 1980, **19**, 332.
- P. C. Steinhardt, W. L. Gladfelter, A. D. Harley, J. R. Fox, and G. L. Geoffroy, *Inorg. Chem.*, 1980, **19**, 332; D. A. Roberts, A. D. Harley, and G. L. Geoffroy, *Organometallics*, 1982, **1**, 1050.
- C. H. Wei and L. F. Dahl, *J. Am. Chem. Soc.*, 1966, **88**, 1821; C. H. Wei, G. R. Wilkes, and L. F. Dahl, *ibid.*, 1967, **89**, 4972; C. H. Wei, *Inorg. Chem.*, 1969, **8**, 2384.
- M. R. Churchill and J. P. Hutchinson, *Inorg. Chem.*, 1978, **17**, 3528.
- B. F. G. Johnson and R. E. Benfield, in 'Topics in Inorganic Chemistry,' ed. G. Geoffroy, Wiley, New York, 1981, p. 253.
- J. A. Connor, in 'Transition Metal Clusters,' ed. B. F. G. Johnson, Wiley, New York, 1980, p. 345.
- A. Strawczynski, R. Ros, and R. Roulet, *Helv. Chim. Acta*, 1988, **71**, 867.
- J. A. J. Jarvis, A. Johnson, and R. J. Puddephatt, *J. Chem. Soc., Chem. Commun.*, 1973, 373; P. G. Jones, A. G. Maddock, M. J. Mays, M. M. Muir, and A. F. Williams, *J. Chem. Soc., Dalton Trans.*, 1977, 1434.
- A. F. Wells, in 'Structural Inorganic Chemistry,' 4th edn., Clarendon Press, Oxford, 1975.
- K. Wade, *Adv. Inorg. Chem. Radiochem.*, 1976, **18**, 67.
- D. F. Shriver and M. A. Drezdson, 'The Manipulation of Air-sensitive Compounds,' 2nd edn., Wiley, New York, 1986.
- R. Della Pergola, L. Garlaschelli, and S. Martinengo, *J. Organomet. Chem.*, 1987, **331**, 271.
- D. Forster, *Inorg. Nucl. Chem. Lett.*, 1969, **5**, 433.
- E. H. Brate and W. Hubel, *Inorg. Synth.*, 1966, **8**, 178.
- C. A. McAuliffe, R. V. Parish, and A. D. Randal, *J. Chem. Soc., Dalton Trans.*, 1979, 1730.
- L. Garlaschelli, P. Chini, and S. Martinengo, *Gazz. Chim. Ital.*, 1982, **112**, 285; R. Della Pergola, L. Garlaschelli, and S. Martinengo, *Inorg. Synth.*, in the press.
- J. A. Collman, R. G. Finke, J. N. Cawse, and J. I. Brauman, *J. Am. Chem. Soc.*, 1977, **99**, 2515.
- K. Farmery, M. Kilner, R. Greatrex, and N. N. Greenwood, *J. Chem. Soc. A.*, 1969, 2339 and refs. therein.
- B. A. Frenz and Associates, SDP Plus Version 1.0, Enraf-Nonius, Delft, 1980.
- A. C. T. North, D. C. Phillips, and F. S. Mathews, *Acta Crystallogr., Sect. A*, 1968, **24**, 351.
- 'International Tables for X-Ray Crystallography,' Kynoch Press, Birmingham, 1974, vol. 4.

Received 17th February 1989; Paper 9/00758J